

# 1 SUSY Searches in Multi-Lepton Final States with the ATLAS 2 detector

3 S. MARTIN-HAUGH<sup>(1)</sup> ON BEHALF OF THE ATLAS COLLABORATION

4 <sup>(1)</sup> *University of Sussex, Brighton, UK*

**Summary.** — Searches for the production of supersymmetric particles in proton-proton collisions with the ATLAS detector at the LHC were performed with  $13.0 \text{ fb}^{-1}$  of data collected at  $\sqrt{s} = 8 \text{ TeV}$ . Different final states containing exactly three, or at least four light leptons ( $\ell = e, \mu$ ) were considered. In the absence of any excess, limits were set in several different supersymmetric models.

PACS 12.60.Jv – Supersymmetric models.

5

## 6 1. – Introduction

7 Supersymmetry (SUSY) is one of the best motivated extensions to the Standard  
8 Model, providing a possible solution to the hierarchy problem and a viable dark matter  
9 candidate: a pedagogical introduction is provided in [1]. SUSY models can either con-  
10 serve or violate  $R$ - or matter-parity: examples of both scenarios are considered here. Two  
11 searches for SUSY with the ATLAS detector [2] are discussed here, and are documented  
12 fully in [3] and [4].

13 These searches are interpreted in terms of *simplified models* [5, 6]. Instead of postulating  
14 an entire mass spectrum and associated phenomenology, these models set the masses of  
15 a small number of SUSY particles and use simple choices for branching ratios. Simplified  
16 models cannot be realised in nature, but allow for easy re-evaluation of results under  
17 changing assumptions.

## 18 2. – Three lepton final states: Searches for direct gaugino production

19 Direct searches for coloured SUSY particles at the LHC have set bounds of  $> 1 \text{ TeV}$   
20 on squark and gluino masses in a variety of scenarios. It is possible that weakly produced  
21 particles could be the only supersymmetric particles observable at the LHC. Gauginos  
22 are linear combinations of Higgs and  $W/Z$  boson superpartners, the higgsinos and winos.  
23 Gauginos are then classified (in order of increasing mass) as *charginos* ( $\tilde{\chi}_1^\pm, \tilde{\chi}_2^\pm$ ) and  
24 *neutralinos* ( $\tilde{\chi}_1^0, \tilde{\chi}_2^0, \tilde{\chi}_3^0, \tilde{\chi}_4^0$ ). The cross sections for gaugino production are much lower  
25 than those for strong particle production, and are generally similar to those of electroweak

26 processes such as diboson production. In this analysis, two simplified models are used to  
 27 interpret the results: both model direct  $\tilde{\chi}_1^\pm \tilde{\chi}_2^0$  production. Model 1 (shown in Figure 1a)  
 28 is constrained to have intermediate decays via sleptons and sneutrinos, while in Model  
 29 2 (shown in Figure 1b), the gauginos decay via  $W$  and  $Z$  bosons. Both models conserve  
 $R$ -parity. Since the kinematics of Models 1 and 2 are different, different selection criteria

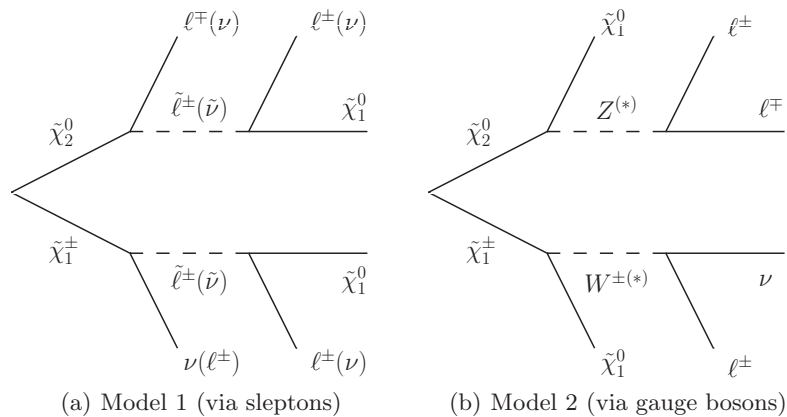


Fig. 1. – Illustration of  $\tilde{\chi}_1^\pm \tilde{\chi}_2^0$  production and decay to three lepton final states.

30 (signal regions) are applied: these requirements are summarised in Table I.  $R$ -parity  
 31 conserving neutralino decays always yield same flavour opposite sign (SFOS) lepton pairs:  
 32 at least one such pair is therefore required in all signal regions. Signal regions are then  
 33 divided into SR1a/b, which veto  $Z$  candidates, and SR2, where a  $Z$  boson candidate is  
 34 required. A  $Z \rightarrow \ell\ell$  candidate is defined as a SFOS pair with invariant mass within 10  
 35 GeV of  $m_Z$ . Jets identified as originating from  $b$ -quarks ( $b$ -tagged jets) are vetoed in  
 36 SR1a/b in order to reduce the contribution from  $t\bar{t}$  production. In SR2, a transverse  
 37 mass ( $m_T = \sqrt{2p_T^\ell E_T^{\text{miss}} \cos \Delta\phi_{\ell, E_T^{\text{miss}}}}$ ) cut is applied to reduce the contribution from  
 38  $WZ$  production. The lepton used for the  $m_T$  calculation does not form part of the  
 39 SFOS pair closest to  $m_Z$ .  
 40

Selection	SR1a	SR1b	SR2
Number of leptons ( $e, \mu$ )			Exactly 3
Lepton charge, flavour	At least one SFOS pair and no SFOS pair with $m_{\ell\ell} < 12$ GeV		
Targeted $\tilde{\chi}_2^0$ decay	$\tilde{l}^{(*)}$ or $Z^*$		on-shell $Z$
$Z \rightarrow \ell\ell$ candidate	veto		requirement
Number of $b$ -jets	0		any
$E_T^{\text{miss}}$	$> 75$ GeV		$> 120$ GeV
$m_T$	any	$> 110$ GeV	$> 110$ GeV
$p_T$ of leptons	$> 10$ GeV	$> 30$ GeV	$> 10$ GeV

TABLE I. – Signal regions for the three lepton analysis. All signal regions require exactly three leptons including a same flavour, opposite sign (SFOS) lepton pair. SR1a and SR1b are most effective for Model 1 (via sleptons), while SR1a and SR2 are most effective for Model 2 (via  $W$  and  $Z$  bosons). Taken from Ref. [3].

41 **2.1. Background estimation.** – The different background contributions are classified  
 42 as *irreducible* if they contain at least three real leptons, and as *reducible* if they contain  
 43 fewer than three real leptons. The major irreducible backgrounds are  $WZ$ ,  $ZZ$ ,  $t\bar{t}+W/Z$ ,  
 44  $WWW$ ,  $ZWW$  and  $ZZZ$  production, while the major reducible backgrounds are  $t\bar{t}$ , single  
 45 top,  $Z$  and  $W$  production in association with jets. The predictions for irreducible  
 46 backgrounds are predicted by Monte Carlo (MC) simulations, while experimental data  
 47 is used to predict the reducible background.  $WZ$  is the largest irreducible background  
 48 and is therefore normalised to data in a control region. The observed scale factor for the  
 49  $WZ$  MC is found to be  $1.03 \pm .0.14$ .

50 For the estimation of reducible backgrounds, leptons are categorised as “real” (R) if they  
 51 are produced in  $\gamma^*/Z$ ,  $W$  or SUSY decays, and as “fake” (F) if they come from heavy  
 52 flavour decays or external conversion. The contribution from light flavour jets faking lep-  
 53 tons is found to be negligible for this analysis. Reconstructed leptons are reconstructed  
 54 with “tight” (T) (low efficiency, high purity) or with “loose” (L) (high efficiency, low  
 55 purity) identification level. The vector of possible reconstructed lepton combinations  
 56 ( $N_{TTT}$ ,  $N_{TTL}$ , ...  $N_{LLL}$ ) may be written as a linear combination of real and fake con-  
 57 tributions ( $N_{RRR}$ ,  $N_{RRF}$ , ...  $N_{FFF}$ ), using a matrix  $\mathbf{M}$  of identification efficiencies and  
 58 misidentification probabilities. Inverting the matrix gives an estimate of real and fake  
 59 background contributions. Since the highest  $p_T$  lepton is found to be real in 99% of  
 60 simulated events, the matrix is reduced in size from  $8 \times 8$  to  $4 \times 4$ . The identification  
 61 efficiencies and misidentification probabilities are measured in experimental data.

62 **2.2. Results.** – In order to verify the background prediction, data and MC agreement  
 63 is checked in dedicated validation regions. Good agreement between data and the back-  
 64 ground prediction is observed: distributions and a full table of results may be found in  
 65 Ref. [3]. After this validation process, the data in the signal regions are analysed: the  
 66 results are given in Table II, and the distributions of  $E_T^{\text{miss}}$  in each signal region are  
 67 shown in Figure 2. No significant excess is seen in any of the signal regions.

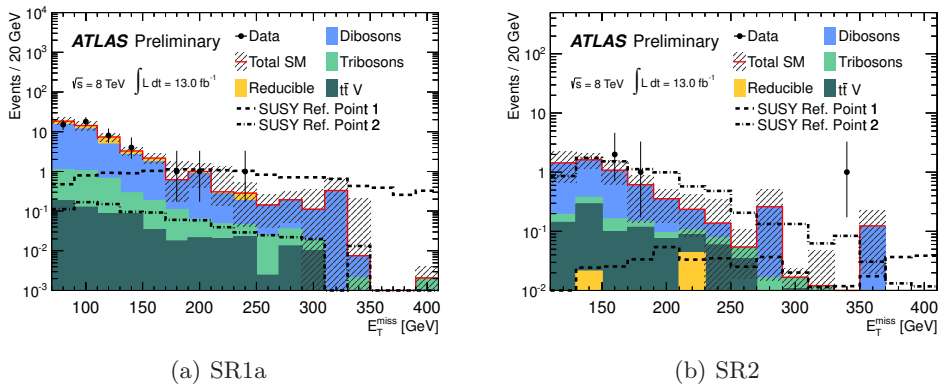


Fig. 2. –  $E_T^{\text{miss}}$  in two of the signal regions used in the three lepton analysis. “SUSY Ref. Point 1” with intermediate sleptons,  $(m_{\tilde{\chi}_1^\pm}, m_{\tilde{\chi}_2^0}, m_{\tilde{\ell}_L}, m_{\tilde{\chi}_1^0} = 500, 500, 250, 0 \text{ GeV})$  and “SUSY Ref. Point 2” with no intermediate sleptons,  $(m_{\tilde{\chi}_1^\pm}, m_{\tilde{\chi}_2^0}, m_{\tilde{\chi}_1^0} = 250, 250, 0 \text{ GeV})$  are also presented. The uncertainty band for the background prediction includes both statistical and systematic uncertainty, while the data uncertainties are statistical only. Taken from Ref. [3].

68 **2.3. Interpretation.** – The visible cross section  $\sigma_{\text{vis}}$  is defined as the total production  
 69 cross section multiplied by the detector acceptance and efficiency.  $\sigma_{\text{vis}}$  is used to constrain  
 70 generic models of new physics. Upper limits at 95% confidence level (CL) on  $\sigma_{\text{vis}}$  are  
 71 shown in Table II. The results are also interpreted as upper limits on the cross sections  
 72 of several SUSY models: all upper limits are derived in the modified frequentist CLs  
 73 formalism [7]. As shown in Figure 3,  $\tilde{\chi}_1^\pm$  and  $\tilde{\chi}_2^0$  with masses up to 580 GeV are  
 74 excluded in the scenario with intermediate slepton decays (Model 1) and masses up to  
 75 290 GeV are excluded in the scenario with decays via gauge bosons (Model 2).” In the  
 76 latter model, there are two distinct regions of exclusion: an additional signal region with  
 77 sensitivity to on-shell  $Z$  boson decays and intermediate  $E_T^{\text{miss}}$  would be required in order  
 to bridge this gap.

Selection	SR1a	SR1b	SR2
$t\bar{t}+V$	$0.62 \pm 0.28$	$0.13 \pm 0.07$	$0.9 \pm 0.4$
triboson	$3.0 \pm 3.0$	$0.7 \pm 0.7$	$0.34 \pm 0.34$
$ZZ$	$2.0 \pm 0.7$	$0.30 \pm 0.23$	$0.10 \pm 0.10$
$WZ$ (normalised)	$34 \pm 4$	$1.2 \pm 0.6$	$4.7 \pm 0.8$
Reducible	$10 \pm 6$	$0.8 \pm 0.4$	$0.012^{+1.6}_{-0.012}$
Total expected events	$50 \pm 8$	$3.1 \pm 1.0$	$6.1^{+2.0}_{-1.2}$
Total observed events	48	4	4
Visible cross section (expected)	$< 1.5$ fb	$< 0.4$ fb	$< 0.5$ fb
Visible cross section (observed)	$< 1.3$ fb	$< 0.5$ fb	$< 0.4$ fb

TABLE II. – *Expected and observed numbers of events with  $13.0 \text{ fb}^{-1}$  of data for the three lepton analysis. Errors on the background prediction are statistical and systematic, summed in quadrature. Taken from Ref. [3].*

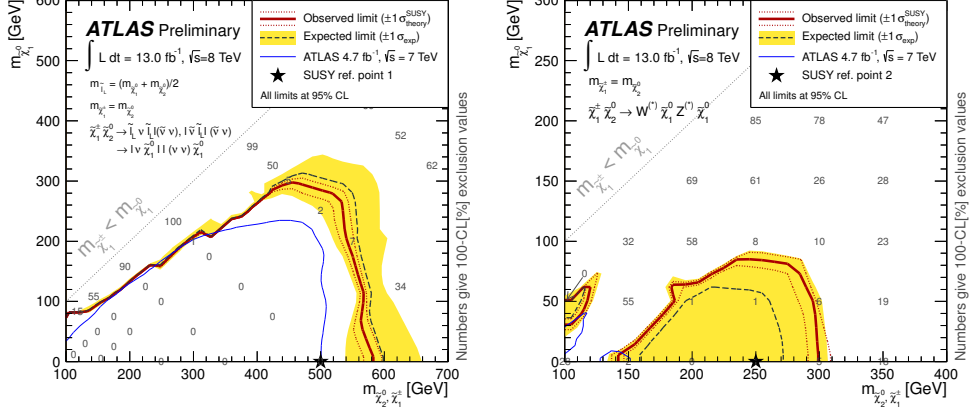
78

### 79 **3. – Four lepton final states: searches for $R$ -parity violating SUSY**

80 In their most general form, SUSY theories contain lepton and baryon number violating  
 81 interactions: the form of such interactions is heavily constrained by the bounds on proton  
 82 decays and similar processes, so  $R$ -parity is often imposed in order to suppress such  
 83 interactions. However, it is possible that a less stringent symmetry is responsible for  
 84 proton symmetry while still allowing lepton and baryon number violating interactions.  
 85 For the models considered in this analysis, lepton number violating SUSY couplings  $\lambda_{ijk}$ ,  
 86 where  $(1, 2, 3) = (e, \mu, \tau)$ , are set to non-zero values. This has the consequence that the  
 87 lightest SUSY particle (LSP) is no longer absolutely stable, but can in fact decay to  
 88 leptons and neutrinos:

$$(1) \quad \tilde{\chi}_1^0 \rightarrow \nu_{i/j} \ell_{j/i}^\pm \ell_k^\mp$$

89 at a rate proportional to  $\lambda_{ijk}$ . Note that for the models considered here, the LSP is  
 90 always the  $\tilde{\chi}_1^0$ . In this analysis, two scenarios are considered: one with  $\lambda_{121} > 0$ , like the  
 91 decay depicted in Figure 4, and one with  $\lambda_{122} > 0$ . In these scenarios, the choice of next-  
 92 to-lightest SUSY particle (NLSP) determines the phenomenology. For each choice of



(a) Model 1: Intermediate decay through slep- (b) Model 2: Intermediate decay through W  
tons and sneutrinos and Z bosons

Fig. 3. – Observed and expected 95% CL limit contours in the two models of direct gaugino production considered here. Both the expected and observed limits are calculated without taking SUSY cross section uncertainties into account. The red dashed band shows the effect of  $\pm 1\sigma$  variation of the SUSY signal uncertainty on the observed limit, while the yellow band shows the effect of  $\pm 1\sigma$  variation of the experimental uncertainties on the final result. Taken from Ref. [3].

93  $\lambda_{ijk}$ , four simplified models of direct NLSP production are considered, with the following  
94 NLSP choices:

- 95 • Wino:  $\tilde{\chi}_1^\pm \rightarrow W^\pm \tilde{\chi}_1^0$
- 96 • Left-handed slepton:  $\tilde{\ell}_L \rightarrow \ell \tilde{\chi}_1^0$
- 97 • Sneutrino:  $\tilde{\nu}_\ell \rightarrow \nu_\ell \tilde{\chi}_1^0$
- 98 • Gluino:  $\tilde{g} \rightarrow q\bar{q}' \tilde{\chi}_1^0$

3.1. *Signal regions.* – Two signal regions are defined: one with high  $E_T^{\text{miss}}$  and one with high  $m_{\text{eff}}$ , where

$$m_{\text{eff}} = E_T^{\text{miss}} + \sum_{\mu} p_T^{\mu} + \sum_e E_T^e + \sum_{\text{jet}} E_T^{\text{jet}}.$$

99 Note that jet and electron  $E_T$  refers to the use of calorimeter information to determine the  
100 momentum: electrons and jets are taken to be massless in the calculation of  $m_{\text{eff}}$ . Selected  
101 RPV decays are expected to have real  $E_T^{\text{miss}}$  from neutrinos, and may additionally have  
102 high  $p_T$  leptons. Decays in the gluino NLSP model can have significant hadronic activity,  
103 motivating the use of  $m_{\text{eff}}$ . Since no on-shell  $Z$  bosons are expected in the models  
104 considered,  $Z$ -candidates are vetoed in all signal regions. The  $Z$ -candidate requirement  
105 is extended to combinations of three or four leptons: the invariant masses  $m(\ell^+ \ell^-)$  (a  
106 single SFOS pair),  $m(\ell^+ \ell^- \ell')$  (an SFOS pair and additional lepton) and  $m(\ell^+ \ell^- \ell'^+ \ell'^-)$   
107 (two distinct SFOS pairs) must all lie 10 GeV from  $m_Z$ .

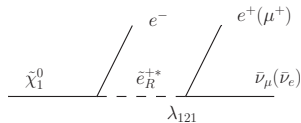


Fig. 4. – Illustration of a  $\lambda_{121} \tilde{\chi}_1^0$  decay. The charge conjugate decay is implied.

108 **3.2. Background estimation.** – Irreducible backgrounds are defined to have at least  
 109 four “real” leptons and zero “fake” leptons, while reducible backgrounds must have at  
 110 least one “fake” lepton. MC simulation is used directly for irreducible backgrounds, while  
 111 a weighting method is used to estimate the reducible background. Leptons are classified  
 112 according to whether they pass the tight requirements ( $\ell_T$ ) or fail the tight requirements,  
 113 but pass the loose requirements ( $\ell_L$ ). The total number of four lepton events with at least  
 114 one fake lepton is then approximated by a single linear equation containing contributions  
 115 from data and MC events with a maximum of two loose leptons. Events with more than  
 116 two fake leptons are found to be negligible in simulation. Relative to the matrix method  
 117 used for the three-lepton analysis (discussed in Section 2.1), the weighting method is  
 118 better suited to the lower statistics of the four lepton analysis.

119 **3.3. Results.** – In order to verify the background prediction, data and MC agreement  
 120 is checked in dedicated validation regions. Good agreement between the data and back-  
 121 ground prediction is observed: distributions and a full table of results may be found in  
 122 Ref. [4]. After this validation process, the data in the signal regions are analysed: the  
 123 results are shown in Table IV. No significant excess is seen in any of the signal regions.

124 **3.4. Interpretation.** – Upper limits on the visible cross section ( $\sigma_{\text{vis}}$ ) at 95% CL are  
 125 derived in both signal regions: the definition of  $\sigma_{\text{vis}}$  and the statistical procedure are  
 126 discussed in Section 2.3. In the absence of excess, these results are interpreted in the  
 127 four simplified models defined: limits in the NLSP-LSP mass plane are shown in Figure  
 128 6 for the case where  $\lambda_{121} > 0$ . The NLSP is excluded for masses up to 700, 400, 450  
 129 or 1300 GeV in scenarios where the NLSP is the wino, L-slepton, sneutrino or gluino  
 130 respectively. The results are also interpreted with  $\lambda_{122} > 0$  in Ref. [4].

Selection	SR1	SR2
Number of leptons		$\geq 4$
Z-candidate		Z-veto
$E_T^{\text{miss}}$	$> 50$ GeV	–
$m_{\text{eff}}$	–	$> 300$ GeV

TABLE III. – The selection requirements for the four lepton signal regions. The Z-candidate veto removes events with either a SFOS lepton pair, a SFOS+l triplet, or a combination of two SFOS pairs with invariant mass within 10 GeV of  $m_Z$ . Taken from Ref. [4].

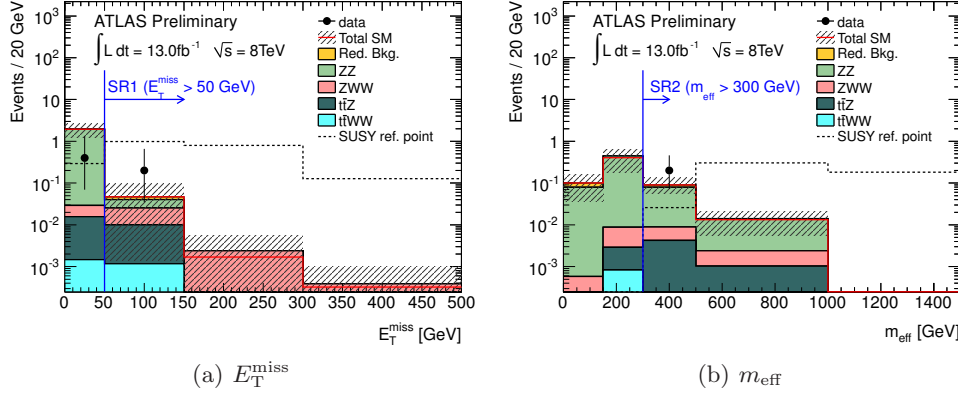


Fig. 5. – Distributions of events with at least four leptons and no  $Z$  boson candidates. Events with  $E_T^{\text{miss}} > 50$  GeV are classified as SR1 (a), while those with  $m_{\text{eff}}$  are in SR2 (b). “SUSY ref. point” is a scenario from the RPV Wino  $\lambda_{121}$  simplified model, with  $m_{\tilde{\chi}_1^\pm} = 600$  GeV,  $m_{\tilde{\chi}_1^0} = 400$  GeV. The uncertainty band for the background prediction includes both statistical and systematic uncertainty, while the data uncertainties are statistical only. Taken from Ref. [4].

#### 131 4. – Conclusion

132 Searches for SUSY in events with exactly three or at least four leptons were  
 133 performed using  $13.0 \text{ fb}^{-1}$  of data recorded at  $\sqrt{s} = 8$  TeV with the ATLAS detector  
 134 in 2012. No significant excess of events above background was observed in either  
 135 analysis, and limits in a variety of different SUSY models were obtained.

#### 136 REFERENCES

137 [1] S. P. Martin, *A Supersymmetry primer*, arXiv:hep-ph/9709356 [hep-ph].

	SR1	SR2
$ZZ$	$0.07^{+0.18}_{-0.08}$	$0.99^{+0.66}_{-0.63}$
triboson	$0.10^{+0.01}_{-0.01}$	$0.08^{+0.01}_{-0.01}$
$t\bar{t}Z$	$0.04^{+0.02}_{-0.02}$	$0.06^{+0.02}_{-0.02}$
$t\bar{t}WW$	$0.01^{+0.01}_{-0.00}$	$0.00^{+0.00}_{-0.00}$
Reducible	$-0.01^{+0.14}_{-0.19}$	$0.09^{+0.17}_{-0.17}$
Total expected events	$0.25^{+0.29}_{-0.25}$	$1.2^{+0.5}_{-0.4}$
Total observed events	1	2
Visible cross section limit (expected)	$< 0.28 \text{ fb}$	$< 0.38 \text{ fb}$
Visible cross section limit (observed)	$< 0.34 \text{ fb}$	$< 0.28 \text{ fb}$

TABLE IV. – Expected and observed numbers of events with  $13.0 \text{ fb}^{-1}$  of data in the four lepton analysis. Errors on the background prediction are statistical and systematic, summed in quadrature. Taken from Ref. [4].

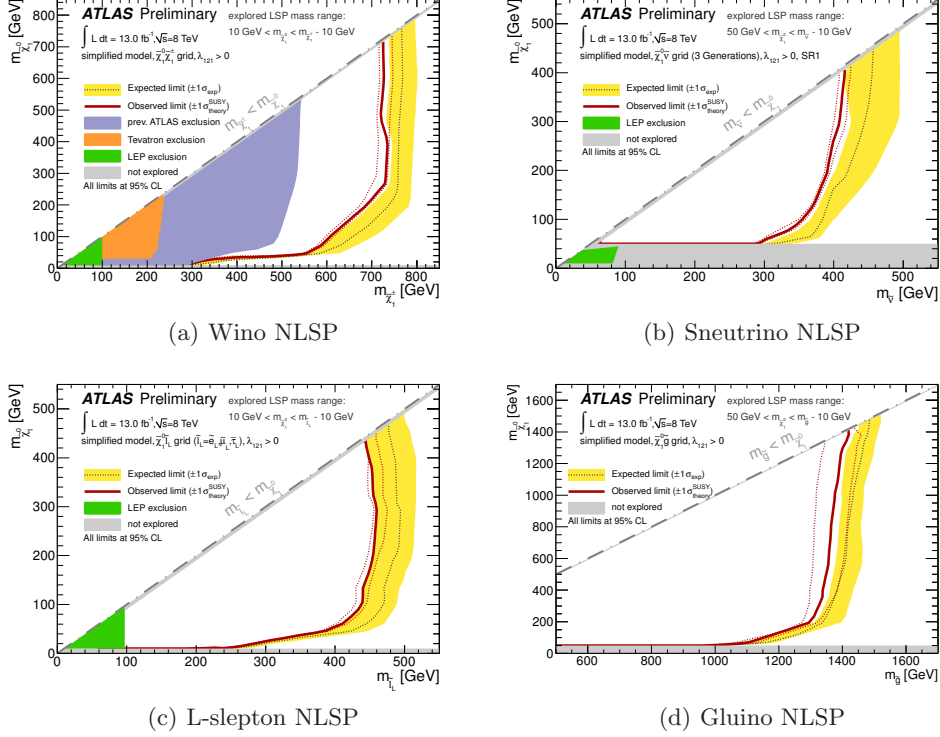


Fig. 6. – Observed and expected 95% CL limit contours in RPV models with the coupling  $\lambda_{121} > 0$ . The chosen NLSP is detailed in the caption. Both the expected and observed limits are calculated without taking SUSY cross section uncertainties into account. The red dashed band shows the effect of  $\pm 1\sigma$  variation of the SUSY signal uncertainty on the observed limit, while the yellow band shows the effect of  $\pm 1\sigma$  variation of the experimental uncertainties on the final result. Taken from Ref. [4].

- 138 [2] ATLAS Collaboration, *The ATLAS Experiment at the CERN Large Hadron Collider*,  
 139 *Journal of Instrumentation* **3** no. 08, (2008) S08003.
- 140 [3] ATLAS Collaboration, *Search for direct production of charginos and neutralinos in events*  
 141 *with three leptons and missing transverse momentum in 13 fb<sup>-1</sup> of pp collisions at*  
 142 *√s = 8 TeV with the ATLAS detector*, Tech. Rep. ATLAS-CONF-2012-154, CERN, Nov,  
 143 2012. <https://cds.cern.ch/record/1493492>.
- 144 [4] ATLAS Collaboration, *Search for supersymmetry in events with four or more leptons in 13*  
 145 *fb<sup>-1</sup> of pp collisions at √s = 8 TeV with the ATLAS detector*, Tech. Rep.  
 146 ATLAS-CONF-2012-153, CERN, Nov, 2012. <https://cds.cern.ch/record/1493493>.
- 147 [5] J. Alwall, P. Schuster, N. Toro *Phys. Rev.* **D79** (2009) 075020.
- 148 [6] LHC New Physics Working Group Collaboration, D. Alves et al., *Simplified Models for*  
 149 *LHC New Physics Searches*, *J.Phys.* **G39** (2012) 105005, [arXiv:1105.2838](https://arxiv.org/abs/1105.2838) [hep-ph].
- 150 [7] A. L. Read, *Presentation of search results: the CL<sub>s</sub> technique*, *Journal of Physics G:*  
 151 *Nuclear and Particle Physics* **28** no. 10, (2002) 2693.